Shock Waves (2023) 33:401–414
https://doi.org/10.1007/s00193-023-01142-5

ORIGINAL ARTICLE

Dual behavior of hydrogen peroxide in gaseous detonations

A. Dahake[1] · R. K. Singh[1] · A. V. Singh[1]

Received: 5 November 2022 / Revised: 15 July 2023 / Accepted: 17 July 2023 / Published online: 27 August 2023

Abstract
The paper describes the dual behavior observed for hydrogen peroxide when added to hydrogen-air detonating mixtures. The effect of the addition of hydrogen peroxide on NO_x emissions and critical detonation parameters was evaluated for H_2 air mixtures using one-dimensional ZND calculations. Hydrogen peroxide acts as an ignition promoter and is shown to significantly enhance the detonation chemistry when added in small concentrations. It alters the ignition chemistry of an underlying detonation wave without affecting the bulk thermodynamic properties. The main objective of the present study is to evaluate the ignition promotion and NO_x mitigation effects of hydrogen peroxide in gaseous detonations when it is added to hydrogen-air mixtures in small and large concentrations. In the current work, the diminishing sensitizing potential of hydrogen peroxide when added in large amounts (up to 10%) is also reported. The results show a visible effect on ignition promotion up to 20,000 ppm. At concentrations higher than 20,000 ppm of H_2O_2, further reduction in the induction length was found to be minimal. The NO_x emissions were found to decrease for stoichiometric and fuel-lean H_2-air mixtures, whereas the NO_x concentration was found to increase for fuel-rich mixtures with the addition of hydrogen peroxide. Thus, the dual behavior exhibited by H_2O_2 is shown to be advantageous as it could potentially mitigate NO_x emissions at high temperatures for fuel-lean and stoichiometric hydrogen-air mixtures and, at the same time, could sensitize the given mixture for applications in detonation-based combustors.

Keywords Detonations · Hydrogen peroxide · NO_x emissions

1 Introduction

Detonations are an efficient way of combusting a fuel-oxidizer mixture and extracting useful work from the chemical energy release [1]. The development of detonation-based propulsive systems is rewarding since such systems offer improved thermodynamic efficiency with reduced mechanical complexity [1–3]. The performance of such propulsive devices depends heavily on the structure of the detonation wave. It is important to address the problems related to the practical applications of such devices. One of the key factors that can influence the implementation of such devices for commercial and propulsion applications is the stringent emissions regulations that need to be followed by these detonation-based devices [4]. There is a pressing need to reduce the anthropogenic carbon footprint, and therefore, the use of biofuels and alternative jet fuels in practical combustion systems is inevitable [5]. The use of carbon-neutral fuels can lower CO_2 emissions. Apart from CO and CO_2 emissions, oxides of nitrogen are also regarded as harmful pollutants in air-breathing propulsion systems [6]. Thus, the mitigation of NO_x emissions from these propulsive devices needs to be addressed.

Gaseous detonations are characterized by extremely high temperatures and pressures, and therefore, it is expected that the NO_x emissions will be higher in a detonating environment since the formation of oxides of nitrogen via the thermal NO_x mechanism will dominate at high temperatures [7]. However, the time and length scales associated with gaseous detonations are significantly lower when compared to a deflagration-based combustion system, which indicates lower NO_x emissions as the gas residence times will be lower in the case of gaseous detonations [7]. The litera-

Communicated by G. Ciccarelli.

✉ A. Dahake
ashlesh@iitk.ac.in

R. K. Singh
ranjay20@iitk.ac.in

A. V. Singh
ajayvs@iitk.ac.in

[1] Department of Aerospace Engineering, Indian Institute of Technology Kanpur, Kanpur, Uttar Pradesh 208016, India

ture on the study of NO_x emissions from detonations or detonation-based propulsive devices is very limited [8–14]. Yungster et al. carried out experimental and numerical work on NO_x emissions from pulse detonation engines fueled by hydrogen and liquid hydrocarbon fuels [8, 9]. For stoichiometric and near-stoichiometric fuel-air mixtures, the NO_x emissions were found to be a strong function of the gas residence times, whereas the NO_x emissions were insensitive to the gas residence times at fuel-lean and fuel-rich conditions [8, 9]. Schwer and Kailasanath numerically carried out a detailed study of the NO_x emission index from detonation tubes and rotating detonation engines [10]. They further studied the effect of different variables (initial pressure (P_0), equivalence ratio (Φ), length, and radius of RDE) on the NO_x emission index of an air-breathing hydrogen-fueled RDE [10]. The experimental data of Ferguson et al. [11] supported Frolov's [7] hypothesis of RDEs having a NO_x advantage due to lower residence times. However, the underlying chemistry of NO_x formation under detonating conditions has not been explored to date. In our recent work, we emphasized the need for using detailed chemical kinetics modeling to study the formation of nitrogen oxides under the harsh conditions of detonation combustion [12–14].

Hydrogen peroxide has been widely studied in combustion systems due to its unique chemical characteristics. It can act as an oxidizer while reacting with other fuels and can also be used as a fuel. The overall decomposition of hydrogen peroxide ($H_2O_2 \rightarrow H_2O + 1/2\ O_2$) is an exothermic process with an energy release of 98.2 kJ/mol, and therefore highly concentrated hydrogen peroxide, also known as high-test peroxide (HTP), can be used for power thrusters [15]. Hydrogen peroxide exists in liquid form at room temperature, and thus its handling and transportation are relatively easy and do not require sophisticated storage and distribution infrastructure [15].

In combustion applications, H_2O_2 is primarily employed as a combustion enhancer to improve combustion stability and in the reduction of nitrogen oxide emissions [15–19]. The studies carried out in the past indicate that hydrogen peroxide can be used to improve the combustion process in practical systems. The interesting behavior of hydrogen peroxide, when added to combustible mixtures, prompted several studies where an attempt was made to understand the underlying chemistry. A systematic study of the effect of hydrogen peroxide on the combustion characteristics and emissions was carried out by Gribi et al., where the authors simulated the oxidation of large hydrocarbon fuel at relevant combustion conditions [15]. Golovitchev et al. performed a numerical simulation with detailed chemistry to study the auto-ignition of methane in the presence of hydrogen peroxide and reported that the addition of hydrogen peroxide in small concentrations reduces the ignition delay time [16]. Methane-air mixtures under atmospheric conditions were also studied by Ting and Reader using the PREMIX code [17]. They found the addition of H_2O_2 resulted in an increase in the burning velocity, specifically for the richer mixtures [17]. A numerical and experimental study was carried out by Chen et al. for premixed methane-air flames, where the effect of H_2O_2 addition on the laminar burning velocity and NO emissions were studied [18, 19]. Hydrogen peroxide has also been used in detonations as an ignition promoter [20–22]. Recently Kumar et al., through their numerical simulations, demonstrated the use of H_2O_2 as an ignition promoter for H_2–O_2/air and C_2H_4–O_2/air mixtures. They showed that it is possible to widen the detonability limits and reduce the operating temperatures of detonation-based propulsive devices with the addition of hydrogen peroxide (up to 15,000 ppm) [21]. Hydrogen peroxide has also been used as an additive to improve the Chapman–Jouguet detonation velocity deficit [23].

All studies reported in the literature to date have primarily pointed out the ignition promotion effects of hydrogen peroxide at lower concentrations due to the generation of hydroxyl radical (OH) during the decomposition of hydrogen peroxide [20, 21, 24]. The effect of H_2O_2 addition to fuel-oxidizer mixtures at higher additive concentrations has still not been reported. Also, no systematic study has been carried out to date to study the effect of H_2O_2 on NO_x emissions under detonation conditions. Very few studies have been conducted in the past for identifying the role of hydrogen peroxide on NO_x emissions from a practical combustion system [15–19]. This is because the effects of hydrogen peroxide on reactive mixtures are not identical since it largely depends on the type of fuel, additives used, and the combustion environment [15–17]. Hydrogen peroxide can be used as a fuel sensitizer for detonation-based propulsive devices [21]. Therefore, it is important to study the effect of H_2O_2 addition on NO_x emissions under detonation conditions.

In the current work, numerical computations were performed to examine the effect of H_2O_2 addition on NO_x emissions and the detonation chemistry of hydrogen-air mixtures. The major objective of the current study is to investigate and evaluate the effect of hydrogen peroxide on NO_x emissions under detonation conditions. The effect of small amounts of H_2O_2 addition to fuel-oxidizer mixtures is very well documented, and the mechanism for the promotion of ignition chemistry is well understood. However, studies in the past have primarily focussed on the role of H_2O_2 as a dopant at lower concentrations and its effect on the various time and length scales of detonations. In such cases, researchers have observed a major promotion effect at smaller doping levels [21, 22]. Therefore, in the present study, we have carried out numerical computations over a wide range of H_2O_2 concentrations (up to 10%) and have studied the effect of the

addition of hydrogen peroxide on the detonation length and time scales and NO_x emissions.

2 Methodology

The Zeldovich–von Neumann–Doring (ZND) detonation model [25–27] was employed in the current work to study hydrogen-air gaseous detonations in the presence of hydrogen peroxide. The numerical computations were carried out using the modified version of the Caltech Shock and Detonation Toolbox (SDT) [28]. The chemical kinetics calculations were carried out using Cantera, an open-source software used to solve problems involving chemical kinetics, transport, and thermodynamics processes [29]. Cantera, along with MATLAB, was also used to calculate the species data for major species and the radicals. The H_2/air chemistry was modeled using the USC Mech II reaction mechanism [30]. The nitrogen oxide formation chemistry was modeled by incorporating the San Diego mechanism [31]. The mechanism is specifically used to model the N_2 chemistry in high-temperature combustion and detonation applications. One of the objectives of the current work is to investigate the ignition promotion effect of hydrogen peroxide at higher concentrations on H_2-air detonations. Therefore, the concentrations of H_2O_2 employed for the numerical computations were such that the change in the critical detonation parameters was less than 5%. The value of 5% was chosen to highlight the change in the detonation parameters is minimal with the addition of hydrogen peroxide, even at large concentrations (up to 10%).

The induction zone length/time is the characteristic length/time scale of a ZND detonation structure. The induction length can be correlated to the detonation cell width, which is the single most prominent detonation parameter [1]. The variation in the induction length is indicative of a corresponding variation in the detonation cell size/width of a multidimensional cellular detonation [32]. The induction zone starts just after the leading shock front and extends till the thermicity peak. The induction zone is a radical generating zone dominated by two-body chain branching reactions with minimal heat release. The corresponding length and time scale is the induction zone length (Δ_i) and induction time (τ_i), respectively. The location of the thermicity peak behind the leading shock also coincides with the maximum temperature gradient. Thus, Δ_i and τ_i can also be defined based on the maximum temperature gradients. The recombination zone follows the induction zone and is dominated by three-body chain termination reactions. The three-body chain termination reactions are exothermic, and therefore most of the heat release occurs in the recombination zone, where a substantial amount of temperature rise can be observed. The corresponding length and time scale is the recombination zone length (Δ_{recom}) and recombination time (τ_{recom}), respectively. The recombination time is the time scale during which the gas particles are at high temperatures, and therefore it can be considered as an indicator of the gas residence time. Thus, τ_{recom} can be used as an appropriate ZND time scale in the study of NO_x emissions for gaseous detonations [12–14]. The reaction zone is the combination of the chain-branching dominated induction zone and the chain-termination dominated recombination zone and extends up to the final phase of exothermic heat release. The corresponding length and time scale is the reaction zone length (Δ_r) and reaction time (τ_r), respectively. The different detonation length and time scales employed in the present study are defined below, and more details regarding the criteria behind the selection of these length/time scales can be found in the literature elsewhere [12],

$$\Delta_i = x|_{\dot{\sigma}_{max}} \tag{1}$$

$$\tau_i = t|_{\dot{\sigma}_{max}} \tag{2}$$

$$\Delta_r = x|_{M=0.9} \tag{3}$$

$$\tau_r = t|_{M=0.9} \tag{4}$$

$$\Delta_{recom} = \Delta_r - \Delta_i \tag{5}$$

$$\tau_{recom} = \tau_r - \tau_i \tag{6}$$

where $\dot{\sigma}_{max}$, M, x, and t denote the maximum thermicity, Mach number in the shock attached frame of reference, post-shock distance and post-shock time, respectively.

The non-dimensional stability parameter (χ) is often used in detonation studies to predict cell regularity [33]. The stability parameter χ used by Ng et al. is sufficiently general and can provide a quantitative description of the stability of detonations, even when complex detailed chemistry is used. The non-dimensional stability parameter is defined as,

$$\chi = \varepsilon \frac{\Delta_i}{\Delta_{r,Ng}} \tag{7}$$

The non-dimensional stability parameter depends on the non-dimensional activation energy (ε) of the induction process and the ratio of the induction zone length to the reaction zone length (main heat release zone length). Ng et al. [33] proposed that the reaction zone length can be defined as,

$$\Delta_{r,Ng} = \frac{u_{CJ}}{\dot{\sigma}_{max}} \tag{8}$$

where $\dot{\sigma}_{max}$ and u_{CJ} denote the maximum thermicity and CJ particle velocity in the shock-attached frame, respectively.

Nitrogen is known to form several oxides; however, in practical combustion systems, nitric oxide (NO), nitrogen dioxide (NO_2), and nitrous oxide (N_2O) are found in large quantities and are therefore deemed as major toxic pollutants [6]. The total NO_x concentration reported in the present work is the sum of individual nitrogen oxides

(NO, NO_2, and N_2O) evaluated at the CJ plane (end of the reaction zone) of a ZND detonation structure where the local flow Mach number reaches unity in the shock-attached frame of reference. However, in practical detonation-based propulsion devices, the products expand after the CJ state as the detonation wave is followed by a Taylor–Zeldovich expansion wave which brings the combustion products to rest behind the CJ plane. The chemistry is not frozen after the CJ plane, and thus the NO_x concentrations can change. Further, the NO formed up to the CJ plane can get oxidized to NO_2 downstream, as reported by Yungster et al. [8, 9].

The computations beyond the CJ state were carried out in the current work using the Caltech Shock and Detonation Toolbox and the Combustion Toolbox [34]. The computations were carried out to evaluate the effect of expansion on the computed nitrogen oxide concentrations at the CJ state. The post-expansion thermodynamic state for hydrogen-air CJ detonation was evaluated using the Caltech Shock and Detonation Toolbox [28]. The computation calculates points on an isentrope and Taylor-Zeldovich expansion behind a CJ detonation. Using the post-expansion state thermodynamic parameters and the CJ state gas composition, the structural evolution of the gas undergoing isentropic expansion was traced. The SP problem (isentropic expansion) in the Combustion Toolbox was utilized to evaluate the post-expansion state gas composition [34].

It would be interesting to see how the current estimates can be extrapolated for working prototypes in the presence of non-uniformities in initial conditions, incomplete mixing, and velocity deficits. In detonations, a range of post-shock conditions exists, high temperatures, pressures behind the overdriven wave at the origin of the detonation cell, and lower temperatures as the shock relaxes [35]. The 1D treatment, i.e., the ZND model, does not capture these physics, but instead, such a treatment can be viewed as a descriptor of the averaged detonation behavior over one full cell cycle. The ZND model is then still a useful construct to understand the detonation cell phenomenon and detonation wave kinetics. A more thorough treatment of the evolution of conditions within a detonation cell is necessary to completely describe the large variations of chemical kinetic rates that can exist within a single detonation cell. This more thorough treatment, however, is beyond the scope of the present work, and the computationally tractable ZND model is utilized in the present study to understand the effect of the addition of hydrogen peroxide on ignition kinetics and NO_x emissions for stoichiometric, fuel-lean, and fuel-rich H_2-air mixtures.

3 Results and discussions

3.1 Effect of H_2O_2 addition on H_2–air detonations

The effect of H_2O_2 addition on the detonation chemistry and the detonation parameters was evaluated by carrying out ZND computations for stoichiometric H_2-air mixtures with varying amounts of molar H_2O_2 concentration. Figure 1 shows the effect of H_2O_2 addition on the induction length/time and the post-detonation parameters. The induction length and time decrease with the addition of hydrogen peroxide, whereas the post-shock temperature (T_{VN}), the post-detonation parameters, such as the post-detonation temperature (T_{CJ}), pressure (P_{CJ}), and the detonation Mach number (M_{CJ}), are negligibly affected (refer to Fig. 1 and Table 1).

The results are consistent with the available literature. It is very well known that the addition of H_2O_2 to a detonating mixture alters the ignition chemistry tremendously by radical proliferation and does not affect the bulk thermodynamic and gas dynamic properties of detonation, as shown in Fig. 1 and Table 1. However, it should be noted that the addition of H_2O_2 reduces the induction length (Δ_i) drastically at lower concentration levels (up to 20,000 ppm). The reduction in the induction length saturates after the initial decrease, and the subsequent decrease is minimal for the higher concentrations of H_2O_2 ($> 2\%$ and $< 10\%$). Thus, the ignition promotion effects of hydrogen peroxide either remain the same or vanishes at higher concentrations under the conditions studied. This is an interesting result since the earlier notion of H_2O_2 acting as an ignition promoter at all concentration levels is not entirely correct.

Hydrogen peroxide decomposes through one of the following reactions under different conditions [36],

$$H_2O_2(+M) \rightarrow OH + OH\ (+M) \tag{9}$$

$$H_2O_2(+M) \rightarrow HO_2 + H\ (+M) \tag{10}$$

$$H_2O_2 \rightarrow H_2O + 1/2\ O_2 \tag{11}$$

$$H_2O_2 + OH \rightarrow H_2O + HO_2 \tag{12}$$

Reaction (9) is the primary H_2O_2 decomposition reaction in high-temperature combustion. Reaction (10) occurs less likely due to the difference in the bond energy required to break the HO–OH and the HOO–H bond. The energy required to break the O–H bond (463 kJ/mol) is much greater than the energy required to break the O–O bond (142 kJ/mol) [36]. The heterogeneous decomposition of H_2O_2 through

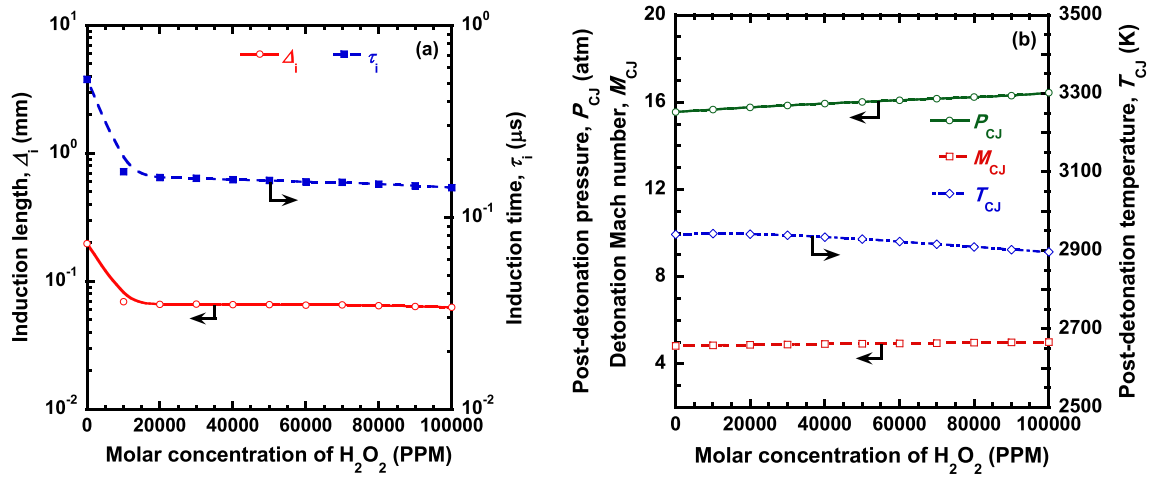

Fig. 1 Effect of H_2O_2 addition on **a** the induction length, the induction time, and **b** the post-detonation parameters of H_2-air detonations. The computations were carried out at $\Phi = 1.0$, $P_0 = 1$ atm, and $T_0 = 298$ K

Table 1 Critical detonation parameters and NO_x concentration for varying hydrogen peroxide concentrations (molar-based) in stoichiometric H_2-air detonations. The computations were carried out at $P_0 = 1$ atm, and $T_0 = 298$ K (X_{sp} denotes the mole fraction of the respective species)

X_{H_2}	X_{air}	$X_{H_2O_2}$ (ppm)	T_{VN} (K)	T_{CJ} (K)	M_{CJ}	Δ_i (mm)	τ_i (μs)	ε	χ	X_{NO} (ppm)	X_{NO_2} (ppm)	X_{N_2O} (ppm)	X_{NO_x} (ppm)
0.296	0.704	0	1529.3	2940.9	4.8	0.1965	0.522	6.37	4.48	240.5	0.118	1.26	241.87
0.294	0.701	5000	1529.0	2942.3	4.8	0.0755	0.190	4.91	1.33	242.9	0.128	1.34	244.4
0.293	0.697	10,000	1528.5	2942.9	4.9	0.0693	0.173	5.04	1.26	243.3	0.138	1.42	244.8
0.290	0.690	20,000	1526.8	2942.1	4.9	0.0658	0.161	5.09	1.20	239.3	0.154	1.57	241.1
0.281	0.669	50,000	1518.7	2929.1	4.9	0.0656	0.155	5.37	1.24	207.5	0.178	1.88	209.6
0.266	0.634	100,000	1502.2	2896.6	5.0	0.0625	0.143	5.73	1.22	146.1	0.174	2.10	148.4

Reaction (11) occurs readily at the reactor surface/chamber walls and is the predominant reaction at temperatures below 400 °C. The attack of OH radical on H_2O_2 results in the formation of the HO_2 radical through Reaction (12), but the reaction is only important at large initial concentrations of hydrogen peroxide [36].

The primary mechanism responsible for the ignition promotion effects of hydrogen peroxide is the rapid decomposition of H_2O_2 to the hydroxyl radical (OH) through Reaction (9), which speeds up the chain branching reactions, thereby reducing Δ_i and τ_i for a given fuel-air mixture. It is known that smaller induction length/time scales represent a tighter coupling between the reaction zone and the leading shock front and quantitatively represent mixtures that are more detonable.

At large concentrations, hydrogen peroxide also reacts with hydroxyl radicals and results in the formation of a relatively stable hydroperoxyl radical (HO_2) and H_2O (through Reaction (12)). The addition of H_2O_2 at 50,000 ppm results in a larger production of HO_2 radicals and an earlier production of H_2O, as shown in Figs. 2c and 3d. HO_2 is produced primarily through Reaction (12) by the consumption of OH radicals by hydrogen peroxide. The more active OH radical is consumed to form H_2O and HO_2 via Reaction (12). Reaction (12) is the primary source of HO_2 production in H_2-air mixtures doped with hydrogen peroxide (at higher concentrations) [36]. The consumption of OH radicals through Reaction (12) will lead to the depletion of OH radicals from the radical pool formed via Reaction (9), thus nullifying the sensitization effect of hydrogen peroxide. The concentration of HO_2 radicals is increased by more than an order of magnitude at 50,000 ppm of H_2O_2, as shown in Fig. 2c. Therefore, the addition of hydrogen peroxide at high concentrations leads to the increased production of OH radicals as well as the HO_2 radical (through Reactions (9) and (12), respectively). This can also be seen in Figs. 2a, 3a, d. Also, the increase in the concentration of HO_2 radicals is higher when compared to OH, H, and O radicals when H_2O_2 is added at large concentrations. The production of hydroxyl radicals (OH) via Reaction (9) is responsible for the ignition promotion effect of H_2O_2. On the other hand, Reaction (12) is responsible for the scavenging of active radicals such as OH. The smaller concentration of H_2O_2 leads to a small amount of HO_2 production, and therefore the chain branching Reaction (9) dominates Reaction (12). At higher H_2O_2 concentrations, the increase in the OH radical production

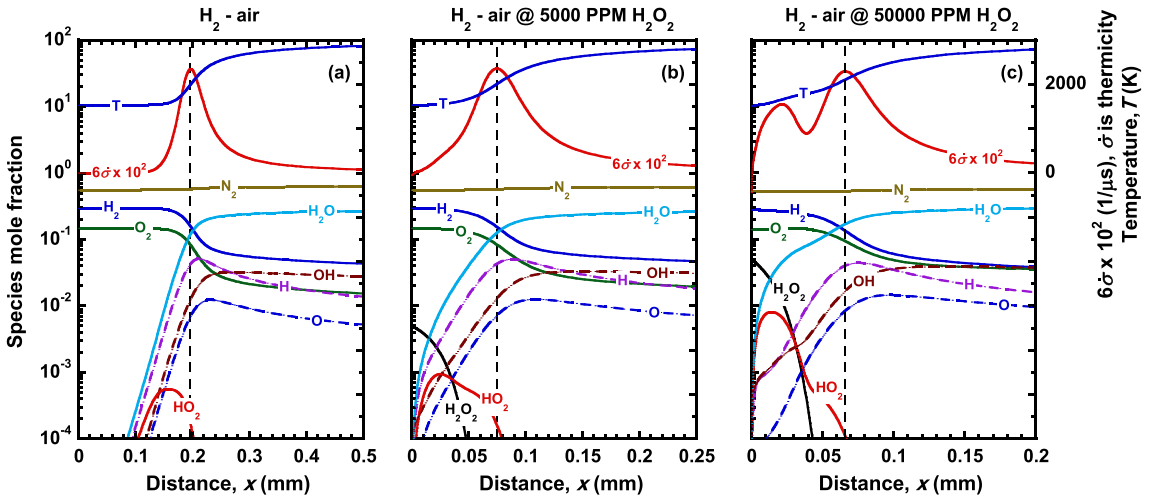

Fig. 2 Species profiles for major species in H_2-air detonation: **a** no dopant, **b** 5000 ppm of H_2O_2, and **c** 50,000 ppm of H_2O_2. The computations were carried out at $\Phi = 1.0$, $P_0 = 1$ atm, and $T_0 = 298$ K

is small when compared to the HO_2 radical production (refer to Figs. 2 and 3a, d). Therefore, at higher concentrations of hydrogen peroxide, the production of the HO_2 radical increases through Reaction (12). Subsequently, Reaction (12) results in the scavenging of active free radicals. The cumulative effect of the competition between Reactions (9) and (12) can explain the small variation in induction length and time scales at higher concentrations of hydrogen peroxide. Thus, the sensitization potential of hydrogen peroxide remains approximately the same at higher concentrations (>20,000 ppm) for H_2-air mixtures, as observed in the current study.

Figure 2 illustrates the profiles of key species for three different cases of H_2-air detonating mixtures. The spatial coordinate is the distance behind the leading shock front. The thermicity curve and temperature profile of a standard ZND structure is also shown in the figure. The peak of the thermicity curve marks the end of the induction zone. Figure 2b, c depict the cases of hydrogen peroxide addition at 5000 ppm and 50,000 ppm molar concentration, respectively. In Fig. 2c (50,000 ppm H_2O_2), two thermicity peaks can be observed; however, a single thermicity peak can be observed in Fig. 2a, b. The first peak in Fig. 2c is due to the intense heat release from Reaction (12), and the second peak corresponds to the heat released during fuel oxidation. Reaction (12) is an exothermic reaction, whereas Reaction (9) is an endothermic reaction. This explains why no double thermicity peaks are observed at lower H_2O_2 addition levels. The addition of H_2O_2 leads to an increase in the production of OH and HO_2 radicals, as discussed and can be seen from Fig. 2b, c. It can be observed that the consumption of O_2 reduces with the increasing concentration of H_2O_2 (refer to Fig. 2a–c). It suggests that H_2O_2 also acts as an oxidizer at higher concentrations. It should also be noted that the H_2O formation starts early in the case of the H_2O_2-doped mixtures primarily due to Reaction (12) and also indicates that the fuel oxidation starts very early for the mixtures doped with hydrogen peroxide.

Figure 3 shows the production and consumption of major radical species such as OH, H, O, and HO_2 as a function of the hydrogen peroxide concentration. The concentration of OH radical increases with the addition of H_2O_2. Also, from Fig. 3a, it can be observed that the OH radical concentration peaks in the post-induction zone, where the three-body recombination reactions are dominant. The effect of H_2O_2 addition is entirely different for H radical, where its maximum concentration decreases with increasing H_2O_2 concentration. The H radical concentration peaks at the end of the induction and is consumed thereafter. The O radical is produced in small quantities as compared to the OH and H radicals. The O radical concentration also increases with increasing H_2O_2 addition, and its concentration peaks just after the induction zone, as shown in Fig. 3c. The production of HO_2 radical under no dopant condition is primarily through the fuel oxidation pathway ($H + O_2(+M) \rightarrow HO_2(+M)$), and therefore it is formed near the flame zone as shown in Fig. 3d. However, with the addition of hydrogen peroxide, specifically at large concentrations, HO_2 is formed before the flame zone through Reaction (12). The formation of HO_2 is also responsible for the dual thermicity peaks, as observed in Fig. 2c, since the formation of HO_2 is an exothermic reaction.

The non-dimensional stability parameter χ is often used in detonation studies to predict cell regularity. Therefore, to explore the effect of H_2O_2 addition on the stability of the detonable mixture, we carried out the stability analysis for all the cases considered in the present work, where we calculated the non-dimensional stability parameter and the activation

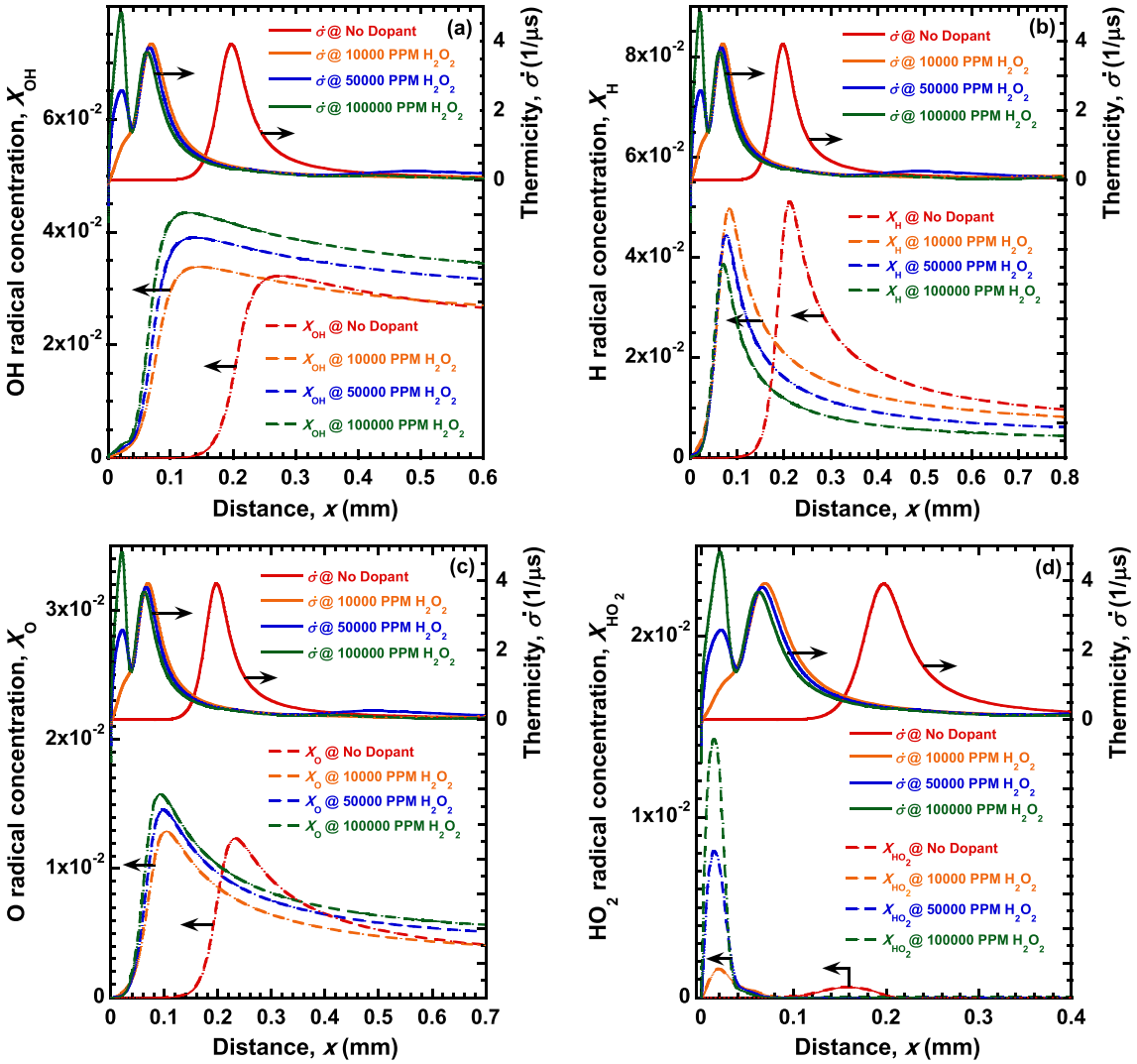

Fig. 3 Species profiles for active radical species with varying concentrations of hydrogen peroxide: **a** OH radical, **b** H radical, **c** O radical, and **d** HO_2 radical. The computations were carried out for H_2-air-H_2O_2 mixtures at $\Phi = 1.0$, $P_0 = 1$ atm, and $T_0 = 298$ K

energy parameter. The computed data is presented in Table 1 and Fig. 4. The stability parameter decreases significantly with the addition of hydrogen peroxide (refer to Table 1 and Fig. 4). With hydrogen peroxide addition, both the activation energy (ε) and the induction zone length Δ_i decreases (refer to Table 1), while the reaction zone length $\Delta_{r,Ng}$ remains fairly constant. Thus, the addition of hydrogen peroxide significantly decreases the stability parameter. It is found that hydrogen peroxide at all concentrations could have a substantial stabilizing effect on the detonation wave structure. Thus, in highly irregular detonations, the addition of hydrogen peroxide could have a stabilizing effect. However, after a steep initial decrease up to 10,000 ppm, the stability parameter remains nearly constant and does not change much. This fact is also supported by our simulations at large concentrations of hydrogen peroxide, where it is found that ignition promotion effects of hydrogen peroxide diminish at large concentration levels. Thus, the sensitization potential of hydrogen peroxide decreases with increasing molar concentration.

It is observed that the normalized activation energy (ε) decreases initially with the addition of hydrogen peroxide up to 10,000 ppm. This is due to the increased production rates of free radicals such as O, OH, and H in the reaction zone in the presence of H_2O_2, which reduce the activation energy. However, at higher concentrations, the reactive radicals such as OH get substituted with a relatively less reactive radical HO_2 ($H_2O_2 + OH \rightarrow H_2O + HO_2$) in the reaction zone. Therefore, the activation energy increases at higher H_2O_2 concentrations. The decrease in the stability parameter, χ, observed with the addition of H_2O_2 is primarily due to a reduction in Δ_i of a ZND detonation structure. The decrease in the induction length significantly affects the ratio $\Delta_i/\Delta_{r,Ng}$, and therefore, a continuous decrease in the ratio can be observed. Thus, as the decrease in the induction length saturates at higher

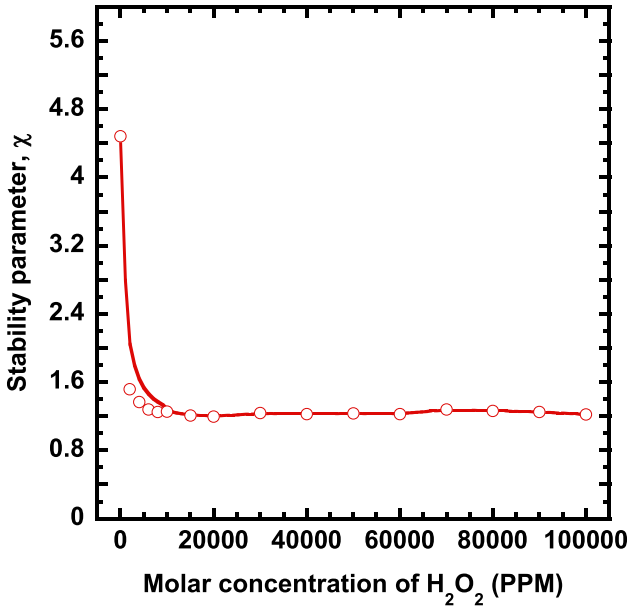

Fig. 4 Effect of molar H_2O_2 addition on the stability parameter for stoichiometric hydrogen-air detonations. The solid line represents a smooth curve fit for the computed data. The computations were carried out at $\Phi = 1.0$, $P_0 = 1$ atm, and $T_0 = 298$ K

H_2O_2 concentrations, similar results were observed for the values of χ. The stability parameter analysis shows that the addition of hydrogen peroxide to H_2-air mixtures could have a stabilizing effect on the resulting detonation wave structure where cell size regularity appears to be affected by both gas dynamics and kinetics. In a previous study [34], detonations were found to be unstable at high values of ε, where the pressure variations in the detonation cells were found to increase with the dimensionless activation energy. Cellular patterns were observed to become sharper with an increase of ε and the regularity of cellular structure was observed to decrease with an increase of ε. Since the addition of hydrogen peroxide up to concentration levels of 10% affects both χ and ε, it is expected that the resulting detonation wave structure and the stability of the wave both get affected by the addition of hydrogen peroxide.

3.2 Effect of H_2O_2 addition on nitrogen oxide emissions from H_2-air detonations

The species profiles are plotted for major NO_x species to highlight the formation of nitrogen oxides in undoped hydrogen-air mixtures. Figure 5 shows nitric oxide (NO) to be the single most abundant NO_x species in hydrogen-air detonations, followed by nitrous oxide (N_2O) and nitrogen dioxide (NO_2), which are formed in substantially lower quantities. For un-doped hydrogen-air mixtures, the maximum concentration of NO was evaluated to be ~240 ppm.

The concentration of other NO_x constituents (N_2O and NO_2) is lower than 2–3 orders of magnitude (see Table 1 and Fig. 5). Also, it can be observed that nitrous oxide is formed before nitric oxide and nitrogen dioxide. The prevalence of nitrous oxide in detonation products has been reported earlier by Frolov et al. [7]. It should also be noted that all the oxides of nitrogen are formed after the induction zone, i.e., in the recombination zone. The formation of oxides of nitrogen takes place in the recombination zone, in which the three-body chain termination reactions are dominant, with the majority of the exothermic heat release. The recombination zone extends up to the CJ plane. Conclusively it should be noted that the nitrogen oxides are formed after an initial induction period. Thus, the chemistry responsible for the formation of NO_x species is completely decoupled from the ignition chemistry for a given fuel-air mixture. Therefore, the induction length/time scale does not affect the formation of NO_x species, and it can be concluded that the NO_x formation chemistry is entirely independent of the induction zone length/time scales. However, in a ZND detonation structure, the recombination time (τ_{recom}) is the time scale that governs the NO_x formation. Thus, τ_{recom} is one of the major factors affecting the formation of oxides of nitrogen. Large recombination zone time scales are indicative of larger gas residence times and thus will lead to the higher formation of NO_x species and vice versa. Thus, in order to evaluate the cumulative effect of hydrogen peroxide addition on NO_x emissions from H_2-air-H_2O_2 detonations, its effect on the post-detonation temperature (T_{CJ}), as well as on the recombination time (τ_{recom}) needs to be effectively investigated.

The total NO_x concentration was evaluated for stoichiometric hydrogen-air mixtures with varying amounts of hydrogen peroxide. The computations were carried out by adding H_2O_2 to stoichiometric H_2-air mixtures. The concentration of NO_x species was evaluated at the CJ plane. The results of the numerical computations are tabulated in Table 1. The overall NO_x concentration decreases with increasing H_2O_2 concentration, as shown in Table 1 and Fig. 6a. It can also be seen that NO is the single most dominant NO_x species amongst the three oxides of nitrogen, and also its molar concentration is more than an order of magnitude higher than NO_2 and N_2O (refer to Table 1 and Fig. 6a). The reduction in NO_x is primarily due to increased NO consumption at higher dopant levels (> 20,000 ppm).

Another reason for the reduction in the concentration of nitric oxide is the reduction in τ_{recom} (refer to Fig. 6b). As discussed earlier, larger values of τ_{recom} favors the formation of NO_x species and vice versa. Therefore, the reduction in recombination time indicates a corresponding reduction in the gas residence times, and thus the production of NO through the thermal NO pathway is hindered, and the concentration of NO_x decreases with increasing H_2O_2 dopant levels. It is observed that nitrous oxide and nitrogen diox-

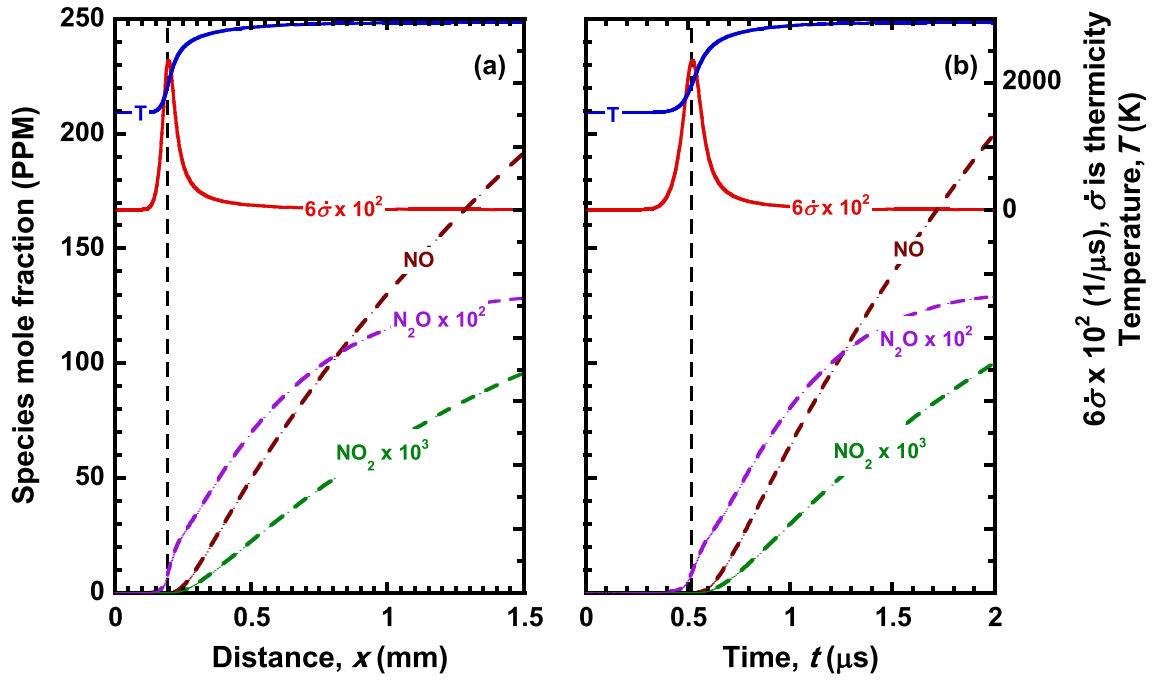

Fig. 5 Thermicity ($\dot{\sigma}$), temperature (T), and species profiles for major NO_x constituents (NO, NO_2, and N_2O) in detonation products for hydrogen-air detonations: **a** spatial scale and **b** temporal scale. The initial conditions, Φ, P_0, and T_0, for the ZND computations were 1.0, 1 atm, and 298 K, respectively

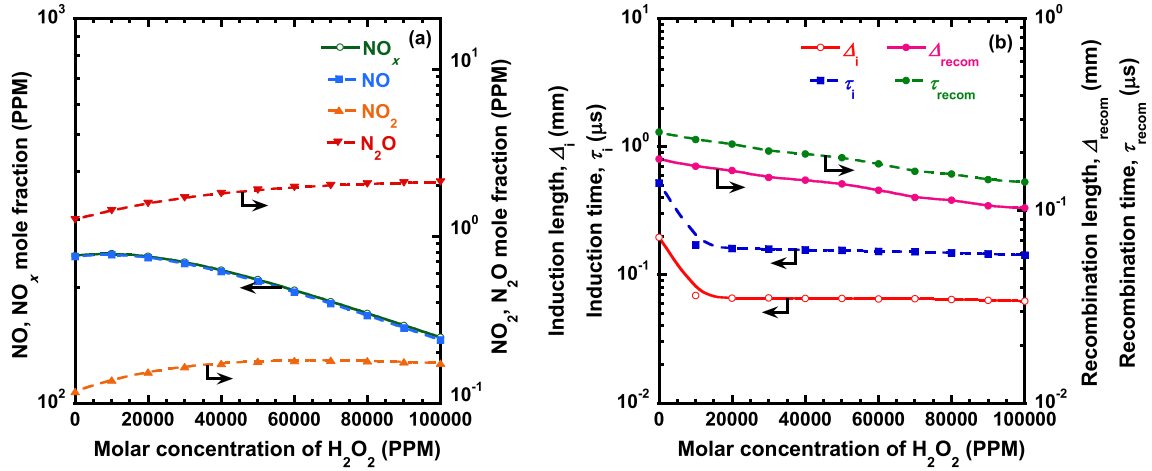

Fig. 6 **a** Variation of the concentration of oxides of nitrogen (NO, N_2O, and NO_2) and the total NO_x concentration with molar H_2O_2 concentration. **b** Variation of detonation length and time scales (Δ_i, Δ_{recom}, τ_i, and τ_{recom}) with molar H_2O_2 concentration. The initial conditions, Φ, P_0, and T_0, for the ZND computations of H_2-air-H_2O_2 mixtures, were 1.0, 1 atm, and 298 K, respectively

ide production increases in the presence of H_2O_2 at all concentrations studied in the current work. However, their concentrations are small, and thus, the concentration of NO_x is primarily governed by NO. Since NO concentration decreases with H_2O_2 addition at large concentrations ($> 20{,}000$ ppm), it acts as a NO_x mitigating agent when added to hydrogen-air mixtures.

In order to gain insights into the reaction kinetics, we carried out a detailed sensitivity analysis for the computations carried out in the current work. The reaction sensitivity analysis was carried out at two different H_2O_2 additive concentrations (5000 ppm and 50,000 ppm). The addition of H_2O_2 has an important impact on the sensitivity coefficients of NO formation (see Fig. 7); for the mixtures with H_2O_2, many reactions exhibit large sensitivity coefficients. It can be observed that most of the reactions in the sensitivity spectra have a positive normalized sensitivity coefficient towards NO formation. The formation of nitric oxide by the

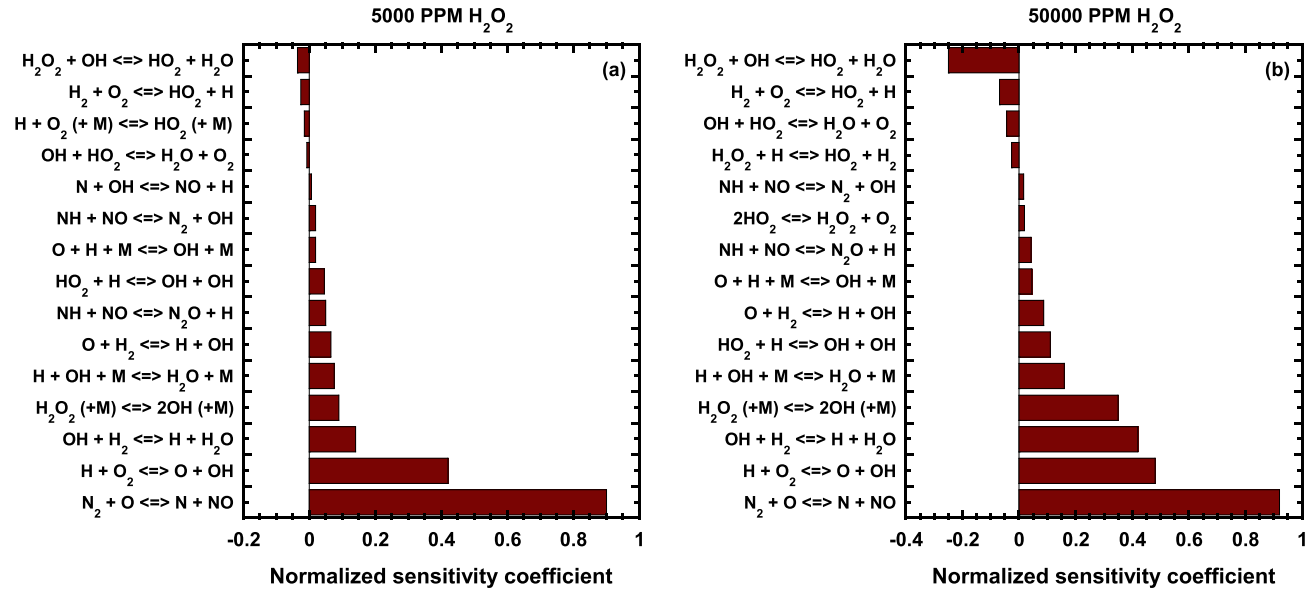

Fig. 7 Ranked sensitivity spectra (top fifteen reactions) for nitric oxide (NO) formation in stoichiometric H_2-air detonations at different H_2O_2 concentration levels: **a** 5000 ppm H_2O_2 and **b** 50,000 ppm. The initial conditions (P_0 and T_0) used for the ZND computations were 1 atm and 298 K, respectively

attack of the oxygen atom on the triple bond of the nitrogen molecule ($N_2 + O \rightarrow NO + N$) exhibits the highest positive normalized sensitivity coefficient. The reactions that facilitate NO formation are typically chain branching in which active radicals are formed. On the other hand, the reactions that hinder NO formation or facilitate NO consumption are chain-terminating. The addition of hydrogen peroxide significantly affects the reaction sensitivity spectra. It can be observed that the normalized sensitivity coefficient for the reaction $H_2O_2 + OH \rightarrow HO_2 + H_2O$ increases drastically as the concentration of hydrogen peroxide increases from 5000 to 50,000 ppm, thereby indicating a strong inhibition action on NO formation (refer to Fig. 7). Interestingly, the reactions showing negative sensitivity towards nitric oxide formation are those which involve the HO_2 radical, such as $H_2O_2 + OH \rightarrow HO_2 + H_2O$, $H_2 + O_2 \rightarrow HO_2 + H$, and $OH + HO_2 \rightarrow H_2O + O_2$. As discussed earlier in the manuscript, the HO_2 radical is formed predominantly at higher hydrogen peroxide concentrations. Therefore, at higher H_2O_2 concentrations, the nitric oxide formation gets hindered. Thus, the addition of hydrogen peroxide results in the overall NO_x reduction, and this NO_x mitigating ability of hydrogen peroxide can be harnessed for reducing the NO_x emissions from practical detonation combustors.

3.3 Dual behavior of hydrogen peroxide

The ignition chemistry of hydrogen-air detonating mixtures was found to be altered in the presence of hydrogen peroxide. The addition of H_2O_2 resulted in radical proliferation, thereby resulting in lower induction zone length/time scales.

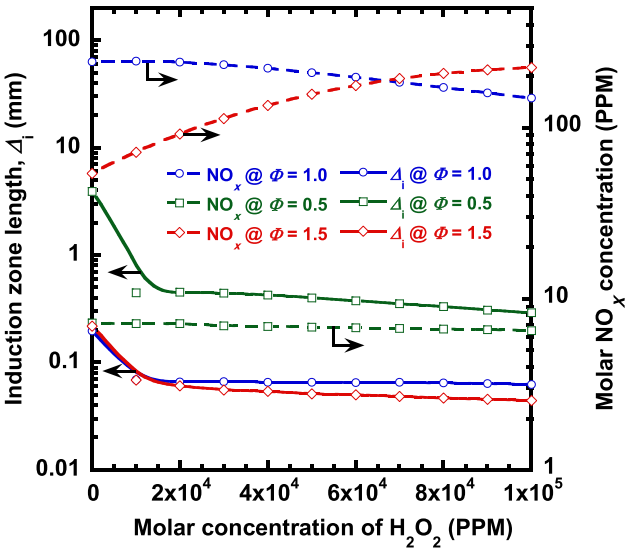

Fig. 8 Effect of H_2O_2 molar concentration on the induction zone length and NO_x for fuel-lean, stoichiometric, and fuel-rich conditions. The computations were carried out for H_2-air detonations at $P_0 = 1$ atm and $T_0 = 298$ K

H_2O_2 addition also resulted in lower overall NO_x emissions, as discussed in previous sections. Thus, H_2O_2 can be used as a NO_x mitigating agent at larger concentrations (> 20,000 ppm) and also as an ignition promoter at all concentrations for stoichiometric H_2-air detonations. Figure 8 shows the variation of the induction length and the overall NO_x concentration with increasing H_2O_2 concentration for fuel-lean, stoichiometric, and fuel-rich conditions.

The induction length decreases with increasing dopant levels; however, the decrease in the induction length scale

Table 2 Detonation properties and NO_x concentration for H_2-air-H_2O_2 gaseous detonation with varying hydrogen peroxide concentration (molar-based) at fuel-lean, stoichiometric, and fuel-rich conditions. The initial conditions, P_0 and T_0, for the ZND computations were 1 atm and 298 K, respectively (X_{sp} denotes the mole fraction of the respective species)

Φ	$X_{H_2O_2}$ (ppm)	X_{H_2}	X_{air}	γ_1	T_{VN} (K)	T_{CJ} (K)	P_{CJ} (atm)	M_{CJ}	Δ_i (mm)	τ_i (μs)	X_{NO_x} (ppm)
0.5	0	0.174	0.826	1.4003	1256.2	2199.6	11.7	4.2	3.92	12.2	7.2
	50,000	0.165	0.785	1.388	1269.2	2234.1	12.3	4.4	0.40	1.1	6.8
	100,000	0.156	0.744	1.376	1280.2	2264.5	13.0	4.5	0.29	0.8	6.5
1.0	0	0.296	0.704	1.4003	1529.3	2940.9	15.6	4.8	0.197	0.52	241.9
	50,000	0.281	0.669	1.388	1518.7	2929.1	16.0	4.9	0.066	0.16	209.6
	100,000	0.266	0.634	1.376	1502.2	2896.6	16.4	5.0	0.063	0.14	148.4
1.5	0	0.387	0.613	1.4003	1525.3	2892.6	15.2	4.8	0.219	0.54	54.1
	50,000	0.367	0.583	1.388	1571.7	3059.7	16.7	5.0	0.051	0.11	156.5
	100,000	0.348	0.552	1.376	1579.0	3111.7	17.5	5.2	0.044	0.09	223.9

is predominant in fuel-lean mixtures (refer to Table 2). Also, it can be observed that the decrease in the induction length is larger for fuel-rich mixtures as compared to the stoichiometric mixtures (see Fig. 8) due to increased post-shock temperature (T_{VN}) (refer to Table 2). The higher temperatures in the induction zone accelerate the chemical kinetics of the fuel-air mixture, and thus a larger decrease in the induction length can be observed for the fuel-rich mixtures. Kumar et al. demonstrated that the use of hydrogen peroxide in fuel-lean mixtures could help in strengthening and stabilizing the detonation wave near its limits [21]. They also showed that operation at fuel-lean conditions could reduce the temperature of the detonation products and can thus widen the operating temperature limits of detonation-based engines.

The addition of hydrogen peroxide to a detonating mixture minimally affects the post-shock pressure (P_{VN}) and temperature (T_{VN}). In the present study, a small change in the post-shock temperature T_{VN} was observed. The T_{VN} increases for fuel-lean and fuel-rich mixtures, whereas it decreases for stoichiometric mixtures with the increase in the concentration of hydrogen peroxide. The post-shock temperature primarily depends on the ratio of specific heats (γ) and the detonation wave Mach number, M_{CJ}. The ratio of specific heats decreases with H_2O_2 addition (1.71% for 10% molar H_2O_2 addition), where the decrease is similar for fuel-lean, stoichiometric, and fuel-rich mixtures. The detonation Mach number increases for fuel-lean, stoichiometric, and fuel-rich H_2-air mixtures. Due to the combined effects of M_{CJ} and, γ the variation in T_{VN} is observed. However, the difference lies in the percentage increase of M_{CJ} since the percentage decrease in γ is the same for fuel-lean, stoichiometric, and fuel-rich mixtures. The M_{CJ} increases by 3.5% for stoichiometric mixtures, whereas it increases by 6.2% and 7.3% for fuel-lean and fuel-rich mixtures, respectively (for 10% molar H_2O_2 addition). This explains why T_{VN} increases with the increase of $X_{H_2O_2}$ at fuel lean ($\Phi = 0.5$) and fuel rich ($\Phi = 1.5$) conditions and decreases at stoichiometric condition ($\Phi = 1.0$). Also, we see the overall change in the T_{VN} with H_2O_2 addition for stoichiometric, fuel-lean, and fuel-rich mixtures is very minimal ($< 4\%$ for all the cases).

Fuel-lean premixed combustion is a widely used NO_x mitigating technique as it reduces the overall NO_x concentration. The reduction of NO_x at fuel-lean conditions is the result of the reduction in the combustion temperatures, thereby retarding the thermal NO_x formation process. However, the fuel-lean operation can lead to instabilities in the resulting detonation wave structure, and the increased cell size could make detonation propagation more difficult. The modest use of H_2O_2 at fuel-lean conditions could alter the ignition chemistry of such mixtures and can help overcome the problems related to the instability and inhibition of the detonation wave. It can also be observed that at lean fuel conditions, the addition of H_2O_2 has a very minimal effect on the total NO_x concentration (see Fig. 8) as the NO_x concentration is already lower under fuel-lean conditions due to reduced detonation temperatures (T_{CJ}) (refer to Table 2).

Hydrogen peroxide addition at higher concentrations to stoichiometric H_2-air mixtures reduce the NO_x emissions from a detonation wave, as shown in Fig. 8 However, in the case of fuel-rich mixtures, the NO_x concentration increases with increasing H_2O_2 concentrations. It is known that for undoped fuel-rich mixtures, the NO_x concentration decreases, primarily due to the decrease in CJ temperatures, which inhibits the thermal NO mechanism. However, in the case of mixtures doped with H_2O_2, the post-detonation temperature increases (refer to Table 2) by more than 200 K. This is because hydrogen peroxide is a strong oxidizer, and thus in fuel-rich conditions, the excess fuel gets oxidized due to the presence of hydrogen peroxide, and thus the detonation temperature increases (refer to Table 2). The thermal NO formation mechanism is very sensitive to temperature changes at elevated temperatures. Thus, the increase in temperature accelerates NO_x formation through the ther-

Table 3 Post-detonation state (CJ state) and post-expansion state thermodynamic parameters and NO_x concentrations for varying hydrogen peroxide concentrations (molar-based) in stoichiometric H_2-air detonations. The computations were carried out at $P_0 = 1$ atm, and $T_0 = 298$ K (X_{sp} denotes the mole fraction of the respective species)

$X_{H_2O_2}$ (ppm)	CJ State			Post-expansion state			Percentage change (%)			
	P_{CJ} (atm)	T_{CJ} (K)	NO_x (ppm)	P_{PE} (atm)	T_{PE} (K)	NO_x (ppm)	$\Delta P = \frac{P_{PE}-P_{CJ}}{P_{CJ}} \times 100\%$	$\Delta T = \frac{T_{PE}-T_{CJ}}{T_{CJ}} \times 100\%$	$\Delta NO_x = \frac{NO_{x,PE}-NO_{x,CJ}}{NO_{x,CJ}} \times 100\%$	
0	15.55	2940.9	241.9	5.80	2584.3	193.1	− 62.70	− 12.13	− 20.17	
5000	15.61	2942.3	244.4	5.83	2587.2	197.4	− 62.65	− 12.07	− 19.23	
50,000	16.02	2929.1	209.6	5.99	2571.3	167.2	− 62.61	− 12.22	− 20.23	
100,000	16.44	2896.6	148.4	6.17	2539.1	116.8	− 62.47	− 12.34	− 21.29	

Subscript *PE* denotes the post-expansion state

mal NO and N_2O mechanisms: $O + N_2 \rightarrow NO + N$, $O + N_2 (+M) \rightarrow N_2O(+M)$, and $N_2O + O \rightarrow NO + NO$. The nitrogen atom in the first reaction is rapidly oxidized to NO by reacting with OH or molecular oxygen (O_2). Nitric oxide at high temperatures could also be formed through the NNH reaction pathway. The H radical combines with N_2 to form NNH through the reaction, $H + N_2(+M) \rightarrow NNH(+M)$. The NNH species formed gets further oxidized to NO through $NNH + O \rightarrow NH + NO$. Therefore, the NO_x concentration is increased with increasing H_2O_2 concentration for fuel-rich mixtures. Thus, as the concentration of H_2O_2 in the fuel-rich mixtures increases, it increases the formation of NO_x species via the thermal NO_x mechanism, which is evident from Fig. 8. Thus, the addition of hydrogen peroxide to H_2-air mixtures shows different effects at different mixture compositions. Increasing the concentration of hydrogen peroxide increases the NO_x concentration for fuel-rich mixtures and decreases it in the case of stoichiometric H_2-air mixtures. However, the NO_x concentration remains fairly constant for fuel-lean mixtures for increased concentrations of hydrogen peroxide.

3.4 NO_x emissions beyond CJ plane

The nitrogen oxide concentrations presented in the previous sections were evaluated at the CJ plane of a ZND detonation structure. It is known that the NO_x concentration levels at the CJ plane are not representative of the realistic NO_x emission levels. The detonation products expand after the CJ state as the detonation wave is followed by a Taylor–Zeldovich expansion wave which brings the combustion products to rest behind the CJ plane. The chemistry is not frozen after the CJ plane, and thus the NO_x concentrations can change. Thus, to evaluate the effect of expansion that follows the CJ detonation on the computed NO_x emissions, further computations were carried out downstream of the CJ plane for H_2-air-H_2O_2 detonations. The calculations were also carried out beyond the CJ plane. The gas composition, as well as the relevant thermodynamic and gas dynamic properties at the CJ state, were chosen as initial conditions for additional calculations beyond the CJ plane. Additional calculations were carried out for an isentropic expansion following the CJ plane to provide a more realistic estimate of the NO_x formation. The calculations were carried out beyond the CJ state up to the post-expansion state, where the plateau conditions were achieved for the gas composition and relevant thermodynamic and gas dynamic properties. The CJ state and post-expansion state parameters and the total NO_x concentration are presented in Table 3.

The addition of hydrogen peroxide to hydrogen-air detonating mixtures minimally affects the post-detonation and post-expansion thermodynamic states. The post-expansion state temperature (T_{PE}) and pressure (P_{PE}) reduce by

$\sim 1.75\%$ and $\sim 6.5\%$, respectively, with the addition of 10% of hydrogen peroxide to hydrogen-air mixtures (refer to Table 3). Thus, the addition of H_2O_2 has a minimal effect on the post-detonation expansion. This is expected due to the fact that the addition of hydrogen peroxide has a significant kinetic effect without affecting the bulk thermodynamic properties of detonating mixture and the detonation products. It can also be observed that the NO_x concentration changes after the CJ state due to the expansion zone following a detonation wave.

The computed NO_x concentration at the end of the expansion zone is lower than the NO_x concentration computed at the CJ plane. The reduction in the total NO_x concentration at the end of the expansion zone is due to the reduction in the pressure and temperature in the expansion zone (refer to Table 3). As the pressure and temperature relax in the expansion wave, the production of NO reduces in the expansion zone. However, it can be seen that the expansion following the CJ state affects the thermodynamic properties and the NO_x concentrations by a similar amount, irrespective of the hydrogen peroxide addition levels. The variation in the thermodynamic parameters and the nitrogen oxide concentration is independent of the presence of hydrogen peroxide in the expansion zone. The pressure, temperature, and NO_x concentration reduce by $\sim 62\%$, $\sim 12\%$, and $\sim 20\%$, respectively, for all H_2O_2 concentrations. The maximum NO_x concentration occurs at the CJ state and decreases further in the expansion zone. The results are consistent with the available literature [10]. From the above calculations, it was found that the expansion that follows the CJ state affects the change in NO by the same amount for all H_2O_2 concentrations. It shows that meaningful extrapolations can be deduced based on the nitrogen oxide concentration at the CJ state, which can give realistic estimates of the NO_x emissions from practical detonation-based devices.

4 Conclusions

The effect of the addition of H_2O_2 to H_2-air mixtures was studied using one-dimensional ZND calculations. Hydrogen peroxide, when added to hydrogen-air mixtures, acts as an ignition promoter at all concentrations. The addition of H_2O_2 to hydrogen-air mixtures reduces the induction length drastically at lower concentration levels (up to 20,000 ppm). At higher concentrations of H_2O_2 ($>20{,}000$ ppm), the subsequent decrease in the induction length is minimal. The overall NO_x concentrations were observed to decrease significantly with the addition of H_2O_2 to stoichiometric H_2-air mixtures. The addition of 10% H_2O_2 (molar concentration) to stoichiometric H_2-air mixtures reduces the NO_x emissions from 241 to 148 ppm ($\sim$ 40% decrease). The NO_x formation chemistry is completely decoupled from the induction zone, and therefore, the reduction in the overall NO_x concentration is primarily due to the consumption of nitric oxide by the pool of OH, H, and O radicals in the post-induction zone. For fuel-lean mixtures, the decrease in NO_x emissions with increasing H_2O_2 concentration was found to be small. On the other hand, it was found that the NO_x emissions increased with increasing H_2O_2 concentration for fuel-rich mixtures because of the strong oxidizing nature of hydrogen peroxide. Thus, hydrogen peroxide acts as a NO_x mitigator at stoichiometric/fuel-lean conditions, whereas it acts as a NO_x promoter at fuel-rich conditions for the cases studied. Thus, hydrogen peroxide acts as an ignition promoter and as a NO_x mitigating agent for stoichiometric and fuel-lean hydrogen-air mixtures at all concentrations. It can be concluded that the addition of hydrogen peroxide to hydrogen-air mixtures has a unique dual behavior where it can be used as an ignition promoter as well as a NO_x inhibitor. The nitrogen oxide emissions from a detonation wave reduce after the CJ plane in the expansion zone due to reduced temperature and pressure. It was also found that the expansion that follows the CJ state affects the change in NO by the same amount for all H_2O_2 concentrations. It shows that meaningful extrapolations can be deduced based on the nitrogen oxide concentration at the CJ state, which can give realistic estimates of the NO_x emissions from practical detonation-based devices. The findings from the current work can be used to harness the unique potential of hydrogen peroxide for applications in detonation-based propulsion devices.

Acknowledgements The financial support from Aeronautics Research and Development Board (ARDB) is gratefully acknowledged for the current work (Grant no. ARDB/01/1042000 M/I).

Data availability All data generated or analyzed during this study are included in this published article.

References

1. Lee, J.H.S.: The Detonation Phenomenon. Cambridge University Press, Cambridge (2008). https://doi.org/10.1017/CBO9780511754708
2. Shepherd, J.E.: Detonation waves and propulsion. In: Buckmaster, J., Jackson, T.L., Kumar, A. (eds.) Combustion in High-Speed Flows. ICASE/LaRC Interdisciplinary Series in Science and Engineering 1, pp. 373–420. Springer, Dordrecht (1994). https://doi.org/10.1007/978-94-011-1050-1_13
3. Kailasanath, K.: Review of propulsion applications of detonation waves. AIAA J. **38**, 1698–1708 (2000). https://doi.org/10.2514/2.1156
4. Anand, V., Gutmark, E.: A review of pollutants emissions in various pressure gain combustors. Int. J. Spray Combust. Dyn. **11**, 1756827719870724 (2019). https://doi.org/10.1177/1756827719870724
5. Dahake, A., Singh, A.V.: A comparative study of the detonation chemistry and critical detonation parameters for Jet A and a bio-derived jet fuel. Trans. Indian Natl. Acad. Eng. **7**(4), 1179–1192 (2022). https://doi.org/10.1007/s41403-022-00353-z

6. Bowman, C.T.: Kinetics of pollutant formation and destruction in combustion. Prog. Energy Combust. Sci. **1**, 33–45 (1975). https://doi.org/10.1016/0360-1285(75)90005-2
7. Frolov, S.M., Basevich, V.Y., Aksenov, V.S., Gusev, P.A., Ivanov, V.S., Medvedev, S.N., Smetanyuk, V.A., Avdeev, K.A., Frolov, F.S.: Formation of nitrogen oxides in detonation waves. Russ. J. Phys. Chem. B **5**, 661–663 (2011). https://doi.org/10.1134/S1990793111040166
8. Yungster, S., Breisacher, K.: Study of NO_x formation in hydrocarbon-fueled pulse detonation engines. 41st AIAA/ASME/SAE/ASEE Joint Propulsion Conference & Exhibit, Tucson, AZ, AIAA Paper 2005-4210 (2005). https://doi.org/10.2514/6.2005-4210
9. Yungster, S., Radhakrishnan, K., Breisacher, K.: Computational study of NO_x formation in hydrogen-fuelled pulse detonation engines. Combust. Theory Model. **10**, 981–1002 (2006). https://doi.org/10.1080/13647830600876629
10. Schwer, D.A., Kailasanath, K.: Characterizing NO_x emissions for air-breathing rotating detonation engines. 52nd AIAA/SAE/ASEE Joint Propulsion Conference, Salt Lake City, UT, AIAA Paper 2016-4779 (2016). https://doi.org/10.2514/6.2016-4779
11. Ferguson, D.H., O'Meara, B., Roy, A., Johnson, K.: Experimental measurements of NO_x emissions in a rotating detonation engine. AIAA SciTech 2020 Forum, Orlando, FL, AIAA Paper 2020-0204 (2020). https://doi.org/10.2514/6.2020-0204
12. Dahake, A., Singh, A.V.: Numerical study on NO_x emissions from a synthetic biofuel for applications in detonation-based combustors. AIAA Propulsion and Energy 2021 Forum, Virtual Event, AIAA Paper 2021-3678 (2021). https://doi.org/10.2514/6.2021-3678
13. Iyer, K.M., Singh, A.V.: NO_x emissions from Jet A-air detonations. AIAA Propulsion and Energy 2021 Forum, Virtual Event, AIAA Paper 2021-3679 (2021). https://doi.org/10.2514/6.2021-3679
14. Dahake, A., Singh, A.V.: Nitrogen oxides emissions from fuel-sensitized detonations for a synthetic biofuel. Trans. Indian Natl. Acad. Eng. **7**(4), 1193–1204 (2022). https://doi.org/10.1007/s41403-022-00354-y
15. Gribi, B., Lin, Y., Hui, X., Zhang, C., Sung, C.J.: Effects of hydrogen peroxide addition on combustion characteristics of n-decane/air mixtures. Fuel **223**, 324–333 (2018). https://doi.org/10.1016/j.fuel.2018.03.054
16. Golovitchev, V.I., Pilia, M.L., Bruno, C.: Autoignition of methane mixtures the effect of hydrogen peroxide. J. Propuls. Power **12**, 699–707 (1996). https://doi.org/10.2514/3.24091
17. Ting, D.S.K., Reader, G.T.: Hydrogen peroxide for improving premixed methane-air combustion. Energy **30**, 313–322 (2005). https://doi.org/10.1016/J.ENERGY.2004.04.039
18. Chen, G.B., Li, Y.H., Cheng, T.S., Hsu, H.W., Chao, Y.C.: Effects of hydrogen peroxide on combustion enhancement of premixed methane/air flames. Int. J. Hydrog. Energy **36**, 15414–15426 (2011). https://doi.org/10.1016/j.ijhydene.2011.07.074
19. Chen, G.B., Li, Y.H., Cheng, T.S., Chao, Y.C.: Chemical effect of hydrogen peroxide addition on characteristics of methane-air combustion. Energy **55**, 564–570 (2013). https://doi.org/10.1016/J.ENERGY.2013.03.067
20. Magzumov, A., Kirillov, I.A., Rusanov, V.D.: Effect of small additives of ozone and hydrogen peroxide on the induction-zone length of hydrogen-air mixtures in a one-dimensional model of a detonation wave. Combust. Explos. Shock Waves **34**, 338–341 (1998). https://doi.org/10.1007/BF02672728
21. Kumar, D.S., Ivin, K., Singh, A.V.: Sensitizing gaseous detonations for hydrogen/ethylene-air mixtures using ozone and H_2O_2 as dopants for application in rotating detonation engines. Proc. Combust. Inst. **38**, 3825–3834 (2021). https://doi.org/10.1016/J.PROCI.2020.08.061
22. Kumar, D.S., Dahake, A., Singh, A.V.: Detonation chemistry of fuel-sensitized Jet al-air detonations. Trans. Indian Natl. Acad. Eng. **7**(3), 957–975 (2022). https://doi.org/10.1007/s41403-022-00339-x
23. Dahake, A., Kumar, D.S., Singh, A.V.: Using ozone and hydrogen peroxide for improving the velocity deficits of gaseous detonations. Trans. Indian Natl. Acad. Eng. **7**(3), 1033–1042 (2022). https://doi.org/10.1007/s41403-022-00345-z
24. Mével, R., Pichon, S., Catoire, L., Chaumeix, N., Paillard, C.-E., Shepherd, J.E.: Dynamics of excited hydroxyl radicals in hydrogen-based mixtures behind reflected shock waves. Proc. Combust. Inst. **34**(1), 677–684 (2013). https://doi.org/10.1016/j.proci.2012.06.151
25. Zeldovich, Y.B.: On the theory of the propagation of detonation in gaseous systems. J. Tech. Phys. **10**, 542–568 (1940)
26. von Neumann, J.: Theory of Shock Waves. World Scientific Publishing Co., River Edge (1943)
27. Döring, W.: On the detonation processes in gases. Ann. Phys. **43**, 421–436 (1943). https://doi.org/10.1002/andp.19434350605
28. Browne, S., Ziegler, J., Shepherd, J.E.: Numerical solution methods for shock and detonation jump conditions. GALCIT Report FM20066, Pasadena, CA
29. Goodwin, D. G., Moffat, H. K., Schoegl, I., Speth, R. L., Weber, B. W.: Cantera: An object-oriented software toolkit for chemical kinetics, thermodynamics, and transport processes. Version 2.6.0 (2022). https://www.cantera.org/
30. Wang, H., You, X., Joshi, A.V., Davis, S.G., Laskin, A., Egolfopoulos, F., Law, C.K.: USC Mech Version II. High-temperature combustion reaction model of H2/CO/C1-C4 compounds (2007). https://ignis.usc.edu:80/Mechanisms/USC-Mech%20II/USC_Mech%20II.htm. Accessed 9 Oct 2021
31. Williams, F.: Chemical kinetic mechanisms for combustion applications. San Diego Mechanism web page, Mechanical and Aerospace Engineering (Combustion Research), University of California at San Diego. http://combustion.ucsd.edu. Accessed 11 Jan 2022
32. Tieszen, S.R., Stamps, D.W., Westbrook, C.K., Pitz, W.J.: Gaseous hydrocarbon—air detonations. Combust. Flame **84**, 376–390 (1991). https://doi.org/10.1016/0010-2180(91)90013-2
33. Ng, H.D., Radulescu, M., Higgins, A., Nikiforakis, N., Lee, J.H.S.: Numerical investigation of the instability for one-dimensional Chapman–Jouguet detonations with chain-branching kinetics. Combust. Theory Model. **9**(3), 385–401 (2005). https://doi.org/10.1080/13647830500307758
34. Cuadra, A., Huete, C., Vera, M.: Combustion Toolbox: A MATLAB-GUI-based open-source tool for solving gaseous combustion problems. V1.0.2 (2023). https://doi.org/10.5281/zenodo.5554911. Accessed 25 Apr 2023
35. Gavrikov, A., Efimenko, A., Dorofeev, S.: A model for detonation cell size prediction from chemical kinetics. Combust. Flame **120**, 19–33 (2000). https://doi.org/10.1016/S0010-2180(99)00076-0
36. Kasper, J.M., Clausen, C.A., III, Cooper, C.D.: Control of nitrogen oxide emissions by hydrogen peroxide-enhanced gas-phase oxidation of nitric oxide. J. Air Waste Manag. Assoc. **46**, 127–133 (1996). https://doi.org/10.1080/10473289.1996.10467444